

# Effect of one ligand substitution on charge transfer and optical properties in *mer*-Alq3: a theoretical study

Ahmad Irfan · Jingping Zhang

Received: 22 June 2009 / Accepted: 19 July 2009 / Published online: 6 August 2009  
© Springer-Verlag 2009

**Abstract** In tris(8-hydroxyquinolato)aluminum (*mer*-Alq3) position for substitution plays an important role. We explain the push–pull effect on the charge transfer and optical properties, if only one of the ligand among three ligands of meridional isomer of *mer*-Alq3 has been substituted. To check this effect, we substituted A-ligand with electron-donating group at position 4 and electron-withdrawing group at position 6. We designed 4-methyl-6-chloro-(8-hydroxyquino)bis(8-hydroxyquinolato)aluminum (**1**), 4-methyl-6-cyano-(8-hydroxyquino)bis(8-hydroxyquinolato)aluminum (**2**), 4-amino-6-chloro-(8-hydroxyquino)bis(8-hydroxyquinolato)aluminum (**3**), and 4-amino-6-cyano-(8-hydroxyquino)bis(8-hydroxyquinolato)aluminum (**4**) derivatives of *mer*-Alq3. All the studied derivatives in the ground ( $S_0$ ) and first excited ( $S_1$ ) states have been optimized at the B3LYP/6-31G\* and CIS/6-31G\* level of theory, respectively. We have designed green light-emitting materials like *mer*-Alq3 and blue light-emitting materials. These derivatives are good candidates for comparable/better charge carrier mobility as *mer*-Alq3.

**Keywords** Organic light-emitting diodes · *mer*-Alq3 · Energy gap · Absorption · Emission · Reorganization energy

**Electronic supplementary material** The online version of this article (doi:10.1007/s00214-009-0616-y) contains supplementary material, which is available to authorized users.

A. Irfan · J. Zhang (✉)  
Faculty of Chemistry, Northeast Normal University,  
130024 Changchun, China  
e-mail: zhangjingping66@yahoo.com.cn

## 1 Introduction

Tang and Van Slyke [1] demonstrated efficient electroluminescence from two-layer sublimated molecular film devices. The development of such devices has progressed significantly over recent years. They are now called organic light-emitting diodes [2], which have high luminescence and efficiency and are easily fabricated. The tris(8-hydroxyquinolato)aluminum (*mer*-Alq3) is a stable aluminum-chelated complex that is one of the most effective organic material used in organic electroluminescent devices [3–11]. The efficiency of charge transport within the organic layer(s) plays a key role. The charge transfer rate can be described by Marcus theory via the following equation [12].

$$W = V^2 / h(\pi / \lambda k_B T)^{1/2} \exp(-\lambda / 4k_B T) \quad (1)$$

There are two major parameters that determine self-exchange electron-transfer rates and ultimately charge mobility: (1) the transfer integral ( $V$ ) between adjacent molecules, which needs to be maximized and (2) the reorganization energy ( $\lambda$ ), which needs to be small for significant transport. The reorganization energy term describes the strength of the electron–phonon (vibration) and can be reliably estimated as twice the relaxation energy of a polaron localized over a single unit.

By introducing the electron-withdrawing (EWD) and electron-donating groups (EDG) into the hydroxyquinoline ligands emissive color can be tuned [13]. In methyl derivatives of *mer*-Alq3 red to blue shifts have been observed by changing the position of substituent in *mer*-Alq3 [14]. In this study our aim is to design high mobility materials having more stability than the parent molecule, thus we substituted A-ligand of *mer*-Alq3 by EDG at position 4 and EWD at position 6 and then reverted the

positions. The present work is in detailed theoretical study, i.e., charge transfer, and optical properties on disubstituted derivatives of *mer*-Alq3 with push–pull (X–Y) substituents (where X = CH<sub>3</sub>/NH<sub>2</sub> and Y = CN/Cl). The 4-X-6-Y-(8-hydroxyquino)bis(8-hydroxyquinolato)aluminum denotes for EDG (X) at position 4 and EWD group (Y) at position 6 on 8-hydroxyquinoline A-ligand.

## 2 Computational details

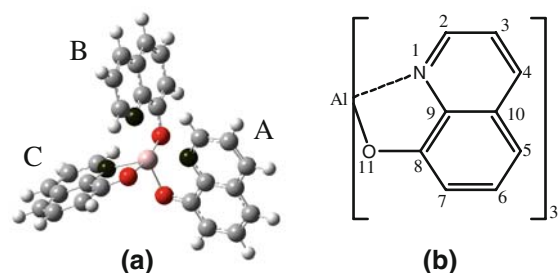
All the calculations have been performed using the Gaussian 03 [15]. Previously we have reported that basis set has no significant effect for *mer*-Alq3 and its derivatives (detail can be found in supporting information). In the ground state (S<sub>0</sub>) molecular geometries have been optimized at the B3LYP/6-31G\* level, which has been proved to be an efficient approach for *mer*-Alq3 and its derivatives [16, 17]. The first excited state (S<sub>1</sub>) geometries have been optimized by configuration interaction with all singly excited determinants (CIS) approach which has been applied by Halls and Schlegel [18]. In our group same approach has been applied on *mer*-Alq3 and its derivatives [17, 19] as well as other OLED materials [20–22], which gave very good and reliable results.

In our previous studies, we have explained that PBE0 gave accurate and reliable absorption and emission energies for *mer*-Alq3 and its derivatives among PBE0, B3LYP, BLYP, SVWN, and B3PW91 functionals. We have also explained that basis set has no significant effect for absorption and emission calculations (see Supporting information). Thus, absorption and emission energies have been calculated by time-dependent density functional theory (TD-DFT) at the PBE0/6-31G\* level [17]. The reorganization energies have been calculated at the B3LYP/6-31G\* level of theory [23].

## 3 Results and discussion

### 3.1 Ground state geometries and electronic structure

Figure 1a is labeled with A–C designating the three different quinolate ligands of *mer*-Alq3. The structure is such that the central Al atom (+3 formal oxidation state) is surrounded by the three quinolate ligands in a pseudo-octahedral configuration with the A- and C-quinolate nitrogens and the B- and C-quinolate oxygens trans to each other. The molecular models used in our calculations, obtained by systematic substitution of CH<sub>3</sub>/NH<sub>2</sub> and CN/Cl in position 4 and 6 on A-ligand, respectively, are shown in Fig. 1b. In Table 1, we have reported selected geometrical parameters of the *mer*-Alq3 and its disubstituted



n	Different ligands	Complexes
4 CH <sub>3</sub> , 6 Cl	4-methyl-6-chloro-(8-hydroxyquino)bis(8-hydroxyquino-linato)aluminum	<b>1</b>
4 CH <sub>3</sub> , 6 CN	4-methyl-6-cyano-(8-hydroxyquino)bis(8-hydroxyquino-linato)aluminum	<b>2</b>
4 NH <sub>2</sub> , 6 Cl	4-amino-6-chloro-(8-hydroxyquino)bis(8-hydroxyquino-linato)aluminum	<b>3</b>
4 NH <sub>2</sub> , 6 CN	4-amino-6-cyano-(8-hydroxyquino)bis(8-hydroxyquino-linato)aluminum	<b>4</b>

n = 4 or 6 denotes as position where “H” was substituted by (CH<sub>3</sub> or NH<sub>2</sub>) and (Cl or CN) on A-ligand as labeled in Figure 1(b)

**Fig. 1** a The geometry of *mer*-Alq3 with labels A–C for three quinolate ligands b the ligand labeling for substituted *mer*-Alq3 complexes considered in this work

**Table 1** Selected optimized bond lengths in angstrom (Å), and bond angles (°) for *mer*-Alq3 and its disubstituted derivatives at the B3LYP/6-31G\* level

Parameters	Alq3	<b>1</b>	<b>2</b>	<b>3</b>	<b>4</b>	Exp <sup>a</sup>
<i>Bond lengths</i>						
Al–N <sub>A</sub>	2.084	2.084	2.079	2.085	2.084	2.050
Al–N <sub>B</sub>	2.126	2.127	2.118	2.128	2.126	2.087
Al–N <sub>C</sub>	2.064	2.063	2.058	2.065	2.063	2.017
Al–O <sub>A</sub>	1.855	1.856	1.857	1.853	1.856	1.850
Al–O <sub>B</sub>	1.881	1.882	1.882	1.879	1.881	1.860
Al–O <sub>C</sub>	1.884	1.885	1.885	1.882	1.885	1.857
<i>Bond angles</i>						
N <sub>A</sub> –Al–N <sub>C</sub>	171.53	171.52	171.41	171.36	171.48	173.82
N <sub>B</sub> –Al–O <sub>A</sub>	172.57	172.67	172.45	172.65	172.61	171.46
O <sub>C</sub> –Al–O <sub>B</sub>	166.56	166.58	166.67	166.34	166.58	168.22

<sup>a</sup> Experimental data of *mer*-Alq3 from [24]

derivatives, where both optimized and experimental results [24] are listed for comparison. Comparative to optimized *mer*-Alq3, the change has not been observed in the Al–N bond lengths of **1**, **3**, and **4** while Al–N bond length of **2** slightly shortened, i.e., 0.008 Å. The change in the Al–O bond lengths has not been found compared to optimized *mer*-Alq3.

The distribution patterns of HOMO, and LUMO of studied derivatives of *mer*-Alq3 in the  $S_0$  states have been shown in Fig. 2. It can be found that the HOMO is localized on A-ligand, and LUMO is on B-ligand in *mer*-Alq3. In 4-methyl-6-chloro-(8-hydroxyquino)bis-(8-hydroxyquinolinato)aluminum (**1**), 4-amino-6-chloro-(8-hydroxyquino) bis(8-hydroxyquinolinato)aluminum (**3**), and 4-amino-6-cyano-(8-hydroxyquino)bis(8-hydroxyquinolinato)aluminum (**4**) HOMO is localized on phenoxide ring of A- and C-ligands while LUMO is on the B-ligand. As far as 4-methyl-6-cyano-(8-hydroxyquino)-bis(8-hydroxyquinolinato)aluminum (**2**) is concerned HOMO is localized on C-, and LUMO is on A-ligand. From Table 2, we have

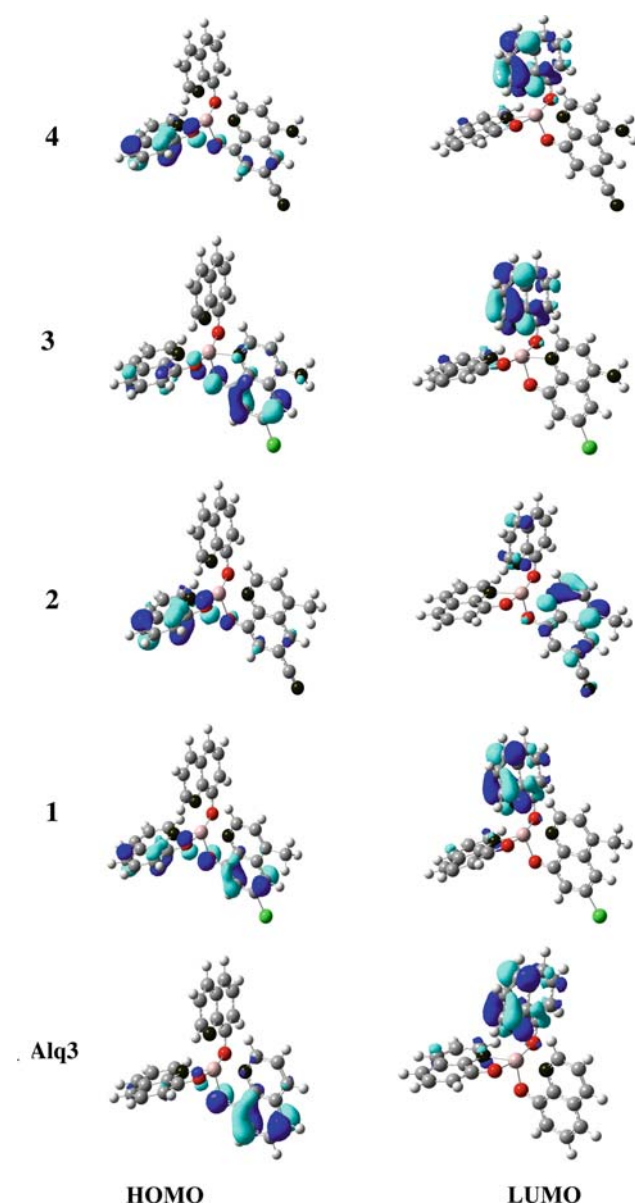


**Fig. 2** Frontier molecular orbitals (FMOs) ( $0.05 \text{ e au}^{-3}$ ) for the ground states ( $S_0$ ) of disubstituted derivatives of *mer*-Alq3

**Table 2** The HOMO, LUMO, and gap energies ( $E_g$ ) in eV computed at the PBE0/B3LYP/6-31G\* level

Complexes	HOMO	LUMO	$E_g$
Alq3	-5.26	-1.65	3.61
<b>1</b>	-5.46	-1.72	3.74
<b>2</b>	-5.60	-1.85	3.75
<b>3</b>	-5.33	-1.64	3.69
<b>4</b>	-5.49	-1.74	3.75

observed that gap energies increased by substituting the EDG and EWD on the positions (the maximum change has been found for **2** and **4**, i. e., 0.14 eV).

### 3.2 The electronic structures of the first excited states

Figure 3 represents the HOMO and LUMO distribution patterns of disubstituted derivatives of *mer*-Alq3 in the excited states ( $S_1$ ). In *mer*-Alq3 and **2**, the HOMO is localized on the phenoxide ring while LUMO is on the pyridyl ring of A-ligand for  $S_1$  states. In **1**, **3**, and **4**, HOMO is localized on the phenoxide ring while LUMO is on the pyridyl ring of B-ligand. The HOMO and LUMO energies of all the four derivatives are smaller than that of *mer*-Alq3. The gap energies are almost same as parent molecule except **2** which has 0.16 eV higher energy gap than that of *mer*-Alq3, see Table 3.

### 3.3 Optical properties

The absorption and emission wavelengths have been computed at the PBE0/6-31G\* level of theory for the disubstituted derivatives, investigated here. In Table 4, we have summarized the calculated and experimental [25] absorption and emission results. All of the four derivatives have the same absorption wavelengths ( $\lambda_a$ ) as *mer*-Alq3. The emission wavelengths ( $\lambda_e$ ) of the studied derivatives revealed that the designed derivatives are green emitting materials except **2** which have the blue emitting properties. Its emission spectra being blue shifted (52 nm) compared to *mer*-Alq3. The blue shift has been observed in **2**, it is due to the increased energy gap (see Sect. 3.2).

### 3.4 Charge transfer properties

The overall relaxation energy consists of two terms which are given by Eqs. 2 and 3.

$$\lambda_{\text{rel}}^{(1)} = E^{(1)}(\text{M}) - E^0(\text{M}) \quad (2)$$

$$\lambda_{\text{rel}}^{(2)} = E^{(1)}(\text{M}^{\pm}) - E^0(\text{M}^{\pm}) \quad (3)$$

Here,  $E^0(\text{M})$  and  $E^0(\text{M}^{\pm})$  are the ground-state energy of the neutral state and the energy of the considered cation/

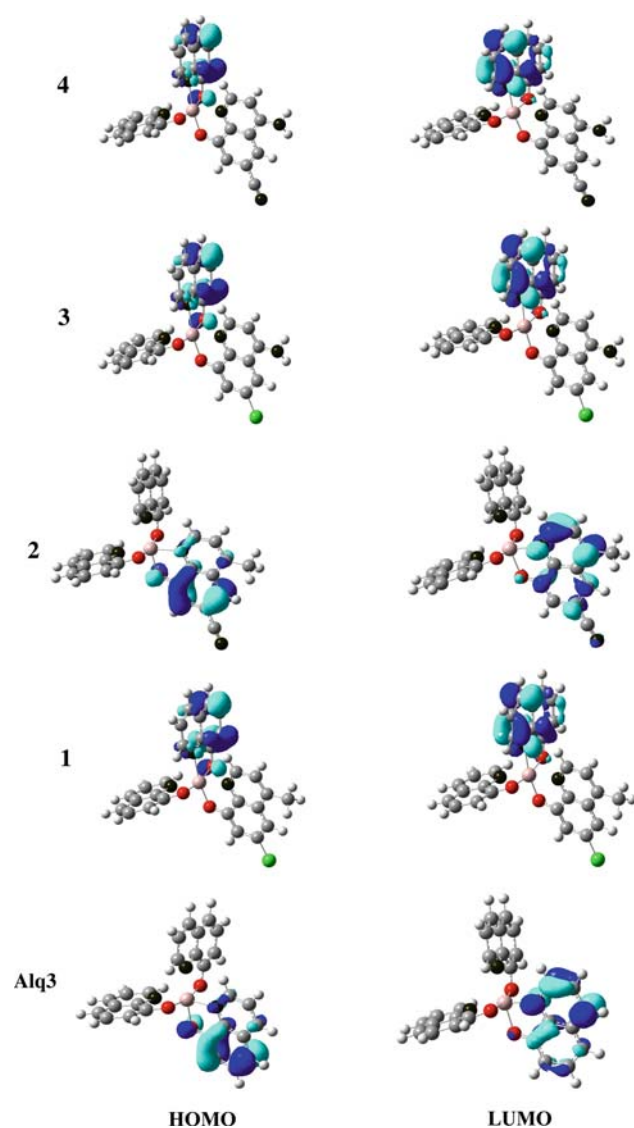


**Fig. 3** Frontier molecular orbitals (FMOs) ( $0.05 \text{ e au}^{-3}$ ) for the excited states ( $S_1$ ) of disubstituted derivatives of *mer*-Alq3

**Table 3** The HOMO, LUMO, and gap energies ( $E_g$ ) in eV computed at the TD-PBE0//CIS/6-31G\* level

Complexes	HOMO	LUMO	$E_g$
Alq3	-4.87	-1.65	3.22
<b>1</b>	-5.20	-1.97	3.23
<b>2</b>	-5.37	-1.99	3.38
<b>3</b>	-5.12	-1.89	3.23
<b>4</b>	-5.21	-1.98	3.23

anion state, respectively;  $E^{(1)}(\text{M})$  is the energy of the neutral molecule at the optimal cation/anion geometry, and  $E^{(1)}(\text{M}^{\pm})$  is the energy of the cation/anion state at the optimal geometry of the neutral molecule.

**Table 4** Calculated absorption and emission wavelengths (nm) of *mer*-Alq3 and its disubstituted derivatives in  $S_0$  ( $\lambda_a$ ) and  $S_1$  ( $\lambda_e$ ) at the TD-PBE0/6-31G\* level

Complexes	$S_0$	exp( $\lambda_a$ )	$S_1$	exp( $\lambda_e$ )
Alq3	410	387	523	515
<b>1</b>	409	–	523	–
<b>2</b>	408	–	471	–
<b>3</b>	412	–	522	–
<b>4</b>	410	–	523	–

exp experimental  $\lambda_a$  and  $\lambda_e$  from [25]

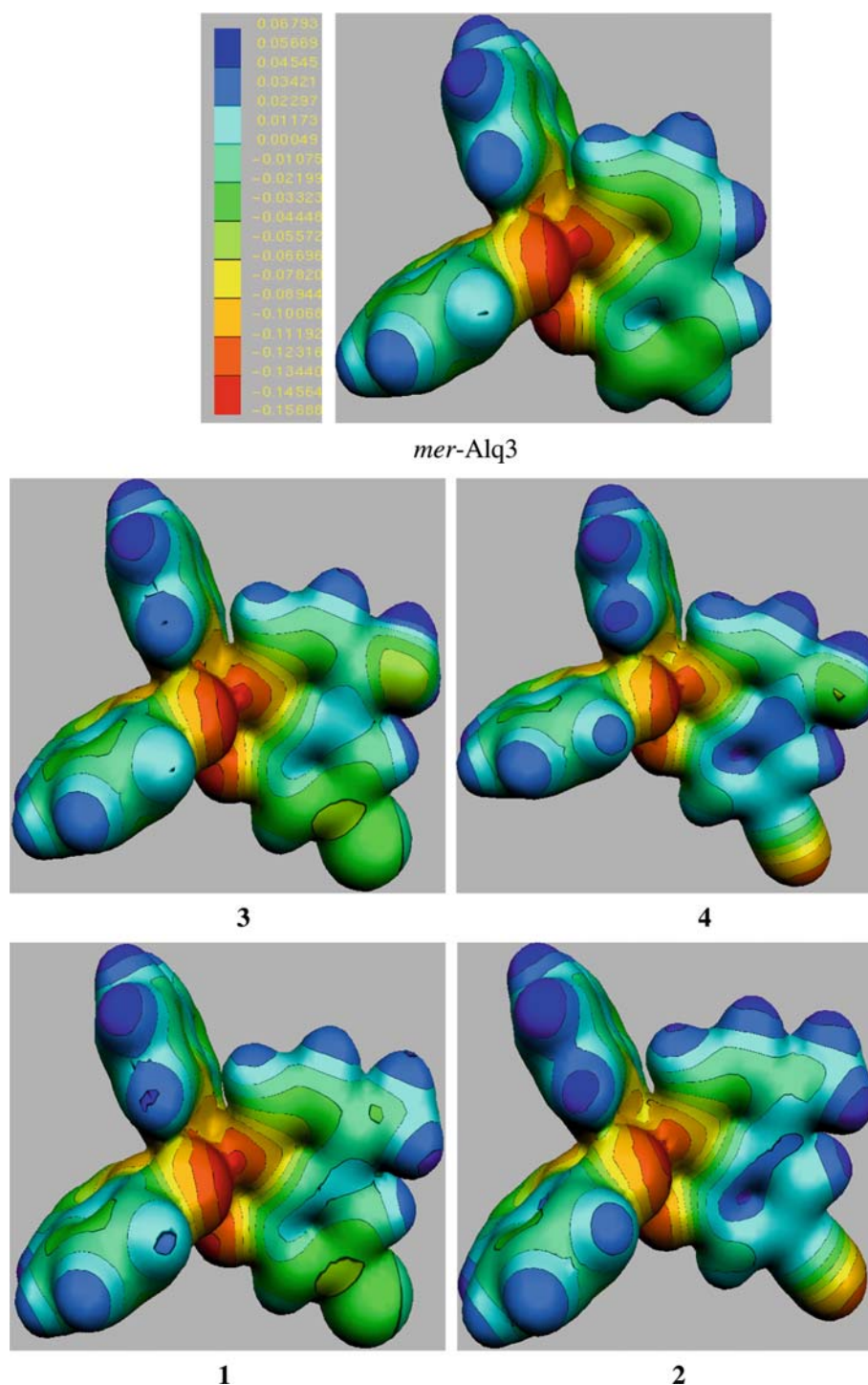
**Table 5** Calculated reorganization energies (in eV) for hole  $\lambda(\text{h})$  and electron  $\lambda(\text{e})$  for *mer*-Alq3 and its derivatives at the B3LYP/6-31G\* level

Complex	$\lambda(\text{h})$	$\lambda(\text{e})$
Alq3 <sup>a</sup>	0.242	0.276
<b>1</b>	0.205	0.225
<b>2</b>	0.136	0.176
<b>3</b>	0.245	0.367
<b>4</b>	0.194	0.245

<sup>a</sup> Alq3 data from [23]

Lin et al. [23] have calculated the internal reorganization energy of *mer*-Alq3 at the B3LYP/6-31G\* level. To compare the results of reorganization energies, we have also calculated the reorganization energies of disubstituted derivatives of *mer*-Alq3 at the same level of theory. From Table 5 it has been found that the reorganization energies for hole and electron of **1**, **2**, and **4** are lower than that of *mer*-Alq3. Among all of the four derivatives **2** has the smallest  $\lambda(\text{e})$  because strongly deactivating group CN is at position 6 and weakly activating group CH<sub>3</sub> is at position 4. In **1** weakly activating -CH<sub>3</sub> and weakly deactivating -Cl groups are at position 4 and 6, respectively. Similarly, in **4** strongly activating group -NH<sub>2</sub> is at position 4 and strongly deactivating group -CN is at position 6. In both the above mentioned cases (**1** and **4**) weakly activating -CH<sub>3</sub> and weakly deactivating -Cl groups (strongly activating group -NH<sub>2</sub> and strongly deactivating group -CN) counterbalance the effect of each other. May be due to this reason no significant change in  $\lambda(\text{e})$  toward small value has been found in these derivatives. The electron reorganization energy of **3** is the highest due to the strongly activating group -NH<sub>2</sub> at position 4 and weakly deactivating group -Cl at position 6. The designed derivatives (**1**, **2**, and **4**) might be good contenders for charge transfer materials. It is expected that EWD substituents may improve the photostability. The **2** and **4** substituted by EWD group -CN decreased the electron

**Fig. 4** Electrostatic surface potentials for *mer*-Alq3 and its disubstituted derivatives. Regions of higher electron density are shown in *red* and of lower electron density in *blue* (values in atomic units)



density in the center of the A-ligand as well as central point of *mer*-Alq3 around Al, which might make oxidation more difficult. The weakly deactivating group -Cl has been substituted in **1** and **3** along with -CH<sub>3</sub> and -NH<sub>2</sub>, respectively (did not decrease the electron density in the central part of the ligand nor in *mer*-Alq3). But one position substitution effect is not so significant (see Fig. 4).

#### 4 Conclusions

We have designed 4-methyl-6-chloro-(8-hydroxyquino)bis(8-hydroxyquinolinato)aluminum (**1**), 4-methyl-6-cyano-(8-hydroxyquino)bis(8-hydroxyquinolinato)aluminum (**2**), 4-amino-6-chloro-(8-hydroxyquino)bis(8-hydroxyquinolinato)aluminum (**3**), and 4-amino-6-cyano-(8-hydroxyquino)bis

(8-hydroxyquinolino)aluminum (**4**) derivatives of *mer*-Alq<sub>3</sub>. In the framework of our present theoretical investigation, we can draw the following conclusions:

- a. The **1**, **3**, and **4** are green light-emitting materials while **2** is blue one.
- b. The electron reorganization energies of **1**, **2**, and **4** are smaller than the parent molecule; dominant decrease in reorganization energy has been observed in **2** where strong deactivating group CN has been substituted.
- c. The newly developed derivatives **1**, **2**, and **4** might have comparable/better charge carrier mobility as *mer*-Alq<sub>3</sub>.
- d. The **2** and **4** might make oxidation more difficult and improve the photostability.

**Acknowledgments** Financial supports from the NSFC 20773022, NCET-06-0321, and NENU-STB07007 are gratefully acknowledged. A. Irfan acknowledges the financial support from China Scholarship Council (CSC) and Ministry of Education (MoE), Pakistan.

## References

1. Tang CW, Van Slyke SA (1987) Appl Phys Lett 51:913
2. Dodabalapur A (1997) Solid State Commun 102:259
3. Tang CW, Van Slyke SA, Cheng CH (1989) J Appl Phys 65:3610
4. Kido J, Kimura M, Nagai K (1995) Science 267:1332
5. Kalinowski J, Di Marco P, Cammaioni N, Fattori V, Stampor W, Duff J (1996) Synth Met 26:77
6. Curioni A, Boero M, Andreoni W (1998) Chem Phys Lett 294:263
7. Sugimoto M, Sakaki S, Sakanoue K, Newton MD (2001) J Appl Phys 90:6092
8. Amati M, Lelj F (2002) Chem Phys Lett 358:144
9. Sun Y, Giebink NC, Kanno H, Ma B, Thompson ME, Forrest SR (2006) Nature 440:908
10. Williams EL, Haavisto K, Li J, Jabbour GE (2007) Adv Mater 19:197
11. Zhang RQ, Lee CS, Lee STJ (2000) Chem Phys Lett 326:413
12. Marcus RA, Sutin N (1985) Biochim Biophys Acta 811:265
13. Curioni A, Andreoni W (2001) IBM J Res Dev 45:101
14. Han YK, Lee SU (2002) Chem Phys Lett 366:9
15. Frisch MJ et al (2004) Gaussian 03, revision B.03, Gaussian, Inc.: Wallingford, CT
16. Irfan A, Cui R, Zhang J (2008) J Mol Struct: Theochem 850:79
17. Irfan A, Cui R, Zhang J, Hao L (submitted)
18. Halls MD, Schlegel HB (2001) Chem Mater 13:2632
19. Gahungu G, Zhang J (2005) J Phys Chem B 109:17762
20. Yang Z, Yang S, Zhang J (2007) J Phys Chem A 111:6354
21. Hu B, Gahungu G, Zhang J (2007) J Phys Chem A 111:4965
22. Sun M, Niu B, Zhang J (2008) J Mol Struct: Theochem 862:85
23. Lin BC, Cheng CP, You ZQ, Hsu CP (2005) J Am Chem Soc 127:66
24. Brinkmann M, Gadret G, Muccini M, Taliani C, Masciocchi N, Sironi A (2000) J Am Chem Soc 122:5147
25. Shi YW, Shi MM, Huang JC, Chen HZ, Wang M, Liu XD, Ma YG, Xu H, Yang B (2006) Chem Comm 18:1941